



The Role of Osmotic Pressure and Tension-Compression Nonlinearity in the Frictional Response of Articular Cartilage

GERARD A. ATESHIAN*, MICHAEL A. SOLTZ, ROBERT L. MAUCK, INES M. BASALO, CLARK T. HUNG and W. MICHAEL LAI

Departments of Mechanical Engineering and Biomedical Engineering, Columbia University, NY 10027-6699, New York, U.S.A.

(Received: 30 November 2000; in final form: 21 December 2001)

Abstract. Articular cartilage is the bearing material of diarthrodial joints such as the knee, hip, or shoulder. Some studies of cartilage lubrication have hypothesized that pressurization of its interstitial fluid may contribute predominantly to reducing the friction coefficient at the contact interface of articular layers. This study introduces a formulation for the dependence of the frictional response of articular cartilage on interstitial fluid pressurization, which accounts for the osmotic pressure in cartilage as well as the tissue's tension-compression nonlinearity, and is based on the theory of mixtures for soft hydrated charged tissues. Theoretical predictions of this model are obtained for the configuration of unconfined compression creep. It is observed from theory that increasing the salt concentration of the tissue's bathing solution reduces the minimum friction coefficient that can be achieved, relative to its equilibrium value; the model also predicts that increasing the applied load can similarly reduce the minimum friction coefficient. Physical interpretations of these phenomena are provided by the model. Experimental results are presented which support these theoretical findings and produce time-dependent responses in good agreement with model predictions. Furthermore, it is observed that the equilibrium friction coefficient does not remain constant under various loads or salt concentrations, and correlation analyses suggest that the equilibrium value depends in part on the compressive strain in the tissue.

Key words: cartilage, osmotic pressure, friction.

1. Introduction

Diarthrodial joints in humans and animals, such as the knee, hip, or shoulder, operate at relatively high loads and low sliding velocities under normal physiologic conditions. Articular cartilage, which lines the ends of the bones at the joint, is its primary bearing material. It exhibits remarkable frictional properties which cannot be explained by traditional lubrication theories, despite the presence of synovial fluid in the joint which had led to early speculations of a fluid film lubrication mechanism (MacConaill, 1932; Dintenfass, 1963; Tanner, 1966; Dowson, 1967).

* Author for correspondence: Tel.: 212-854-8602; Fax: 212-854-3304;
e-mail: ateshian@columbia.edu

Some studies of the biotribology of diarthrodial joints have instead hypothesized that pressurization of the cartilage interstitial fluid may contribute predominantly to reducing the friction coefficient at the contact interface of its articular layers (McCutchen, 1962; Malcom, 1976; Forster *et al.*, 1996; Ateshian, 1997). Indeed, cartilage has a highly hydrated porous permeable matrix (Linn and Sokoloff, 1965; Maroudas, 1979) whose response to mechanical loading can be described by appropriate porous media theories. Using such porous media models, a theoretical formulation describing the dependence of the cartilage friction coefficient on the interstitial fluid pressurization was proposed and verified in an experimental configuration in our recent study (Ateshian *et al.*, 1998). The formulation of this friction model employed the framework of the biphasic theory for soft hydrated tissues (Mow *et al.*, 1980), which models cartilage as a mixture of a solid phase (primarily the collagen-proteoglycan matrix) and a fluid phase (primarily the interstitial water).

From physical chemistry principles however, it is also known that there exists a Donnan osmotic pressure difference between cartilage and its external environment, due to the negatively charged proteoglycans enmeshed within the collagen matrix (Maroudas, 1968, 1979). Theories have been described which combine the solid-fluid mixture approach of the biphasic theory with the presence of a proteoglycan fixed-charge density distribution, such as the electromechanical model of Frank and Grodzinsky (1987), the triphasic theory of Lai *et al.* (1991), the quadriphasic theory of Huyghe and Janssen (1997), and the multiphasic theory of Gu *et al.* (1998). It has been shown experimentally that changes in the ionic content and strength of the bathing solution of cartilage can alter its mechanical (e.g. Maroudas, 1968; Eisenberg and Grodzinsky, 1985; Lai *et al.*, 1991; Basser *et al.*, 1998; Narmoneva *et al.*, 1999) and frictional (McCutchen, 1966; Wright and Dowson, 1976) responses. While the change in mechanical properties has been predicted from theory, the alteration in frictional response, to the extent that it is not just a manifestation of the concomitant change in solid matrix moduli or permeability, remains to be elucidated. Because Donnan osmotic pressure, which contributes to interstitial fluid pressurization of cartilage, can be altered by the ionic environment, its role in the frictional response of cartilage can potentially be significant.

An additional phenomenon that has come to light only recently is that the disparity between the tensile and compressive moduli of articular cartilage acts to enhance the magnitude of interstitial fluid pressurization in compression (Soltz and Ateshian, 2000b). This tension-compression nonlinearity stems from the fibrillar collagenous nature of the solid matrix of articular cartilage, with tensile equilibrium moduli typically ranging from 5 to 40 MPa and compressive equilibrium moduli ranging from 0.1 to 1 MPa. Since the frictional response of cartilage has been hypothesized to be dependent on interstitial fluid pressurization, it is also of interest to incorporate this tension-compression nonlinearity in the formulation of a friction model.

Therefore, the objective of this study is to incorporate both osmotic effects as well as tension-compression nonlinearity of the solid matrix into the formulation of a model to predict the frictional response of articular cartilage; as part of this process, it is necessary to formulate an extension of our prior frictional model in the framework of the triphasic theory. Frictional measurements are also conducted on cartilage samples bathing in NaCl solutions at different strengths, and under different loads, to investigate this mechanism experimentally. The long-term aim of this study is to advance our understanding of cartilage lubrication and the various mechanisms by which this efficient process may potentially be compromised, leading to cartilage degeneration and osteoarthritis.

2. Model Formulation

2.1. BALANCE EQUATIONS

The general derivation of the governing equations for charged-hydrated soft tissues containing multi-electrolytes is given by Lai *et al.* (1991), Huyghe and Janssen (1997), and Gu *et al.* (1998). The model employed here assumes that each phase of the mixture (solid matrix, water, cations, and anions) is intrinsically incompressible and that the mixture is saturated. Only one cation and one anion species of equal valences are considered here, for simplicity (Lai *et al.*, 1991). The continuity equations for all constituents can then be combined into

$$\nabla \cdot \mathbf{v}^s + \nabla \cdot \left[\sum_{\beta=w,+,-} \phi^\beta (\mathbf{v}^\beta - \mathbf{v}^s) \right] = 0, \quad (1)$$

where \mathbf{v}^s is the solid matrix velocity, \mathbf{v}^β are the water solvent ($\beta = w$) and ion ($\beta = +, -$) velocities, and ϕ^β are their corresponding volumetric fractions. For an infinitesimal strain \mathbf{E} and $\phi^+, \phi^- \ll 1$, the mixture saturation condition, $\sum_{\beta=s,w,+,-} \phi^\beta = 1$, leads to the relation

$$\phi^w = [tr(\mathbf{E}) + \phi_\infty^w][1 + tr(\mathbf{E})]^{-1} \cong \phi_\infty^w + (1 - \phi_\infty^w)tr(\mathbf{E}), \quad (2)$$

where ϕ_∞^w is the water volume fraction when the cartilage is in a hypertonic solution, for which $\mathbf{E} = \mathbf{0}$. Since the proteoglycans are fixed to the solid matrix, their fixed-charge density (FCD) given by c^F (Eq/m³ of solvent) similarly relates to its hypertonic configuration value c_∞^F through

$$c^F = c_\infty^F \left[\frac{1 + tr(\mathbf{E})}{\phi_\infty^w} \right]^{-1} \cong c_\infty^F \left[\frac{1 - tr(\mathbf{E})}{\phi_\infty^w} \right]. \quad (3)$$

The momentum equations for the water solvent ($\alpha = w$) and each of the ion constituents ($\alpha = +, -$) are given by

$$-\rho^\alpha \nabla \tilde{\mu}^\alpha + \sum_{\beta=s,w,+,-} f_{\alpha\beta} (\mathbf{v}^\beta - \mathbf{v}^\alpha) = \mathbf{0}. \quad (4)$$

$\tilde{\mu}^\alpha$ is the electrochemical potential of the α th constituent (units of J/kg) and $f_{\alpha\beta}$'s (N.s/m⁴) are the frictional coefficients between the α and β constituents (with $f_{\alpha\beta} = f_{\beta\alpha}$ and $f_{\alpha\beta} = 0$ when $\alpha = \beta$). The apparent density ρ^α (kg/m³) of each ion constituent is related to its concentration c_α (mol/m³ of solvent) and molecular weight M_α (kg/mol) through $\rho^\alpha = \phi^w M_\alpha c_\alpha$, while for the water solvent, $\rho^w = \phi^w \rho_T^w$, where ρ_T^w is the true solvent density. The momentum equation for the whole mixture (2 ion species + solvent + solid = 4 constituents) is given by

$$\nabla \cdot \boldsymbol{\sigma} = \mathbf{0}, \quad (5)$$

where $\boldsymbol{\sigma}$ is the total mixture stress. Electroneutrality of the mixture is satisfied by

$$\sum_{\alpha=+,-} z_\alpha c_\alpha - c^F = 0, \quad (6)$$

where z_α is the algebraic valence of the α th ionic species ($z_+ = +1$, $z_- = -1$). In the absence of electrical current in the tissue (open-circuit configuration), the following relation for the current density must also hold, where F_c is Faraday's constant

$$\mathbf{I}_e = F_c \phi^w \sum_{\alpha=w,+,-} z_\alpha c_\alpha (\mathbf{v}^\alpha - \mathbf{v}^s) = \mathbf{0}. \quad (7)$$

2.2. CONSTITUTIVE RELATIONS

The total stress at any point in the material is given by

$$\boldsymbol{\sigma} = -p\mathbf{I} + \boldsymbol{\sigma}^e, \quad (8)$$

where p is the pressure (inclusive of osmotic effects), \mathbf{I} is the identity tensor, and $\boldsymbol{\sigma}^e$ is the elastic (or effective) stress in the solid phase. To model the tension-compression nonlinearity of the solid matrix, we employ the Conewise Linear Elasticity model of Curnier *et al.* (1995) in its cubic symmetry implementation (Soltz and Ateshian, 2000b),

$$\boldsymbol{\sigma}^e = \sum_{a=1}^3 \left\{ \lambda_1[\mathbf{A}_a : \mathbf{E}] \text{tr}(\mathbf{A}_a \mathbf{E}) \mathbf{A}_a + \sum_{\substack{b=1 \\ b \neq a}}^3 \lambda_2 \text{tr}(\mathbf{A}_a \mathbf{E}) \mathbf{A}_b \right\} + 2\mu \mathbf{E}, \quad (9)$$

which describes a bimodular response (a strain-independent modulus in tension and a strain-independent but different modulus in compression). Here, $\mathbf{A}_a : \mathbf{E} = \text{tr}(\mathbf{A}_a^T \mathbf{E})$ and $\lambda_1[\mathbf{A}_a : \mathbf{E}]$ denotes λ_1 as a function of $\mathbf{A}_a : \mathbf{E}$, where \mathbf{A}_a is a texture tensor corresponding to each of three preferred material directions defined by the unit vectors \mathbf{a}_a , with $\mathbf{A}_a = \mathbf{a}_a \otimes \mathbf{a}_a$ ($\mathbf{a}_a \cdot \mathbf{a}_a = 1$, no sum over a). For cubic material symmetry, $\mathbf{a}_a \cdot \mathbf{a}_b = 0$ when $b \neq a$, and the three directions are generally taken to

be: \mathbf{a}_1 parallel to the split line direction, \mathbf{a}_2 perpendicular to the split line direction, and \mathbf{a}_3 normal to the articular cartilage surface. The term $\mathbf{A}_a : \mathbf{E}$ represents the component of normal strain along the preferred direction \mathbf{a}_a . Tension-compression nonlinearity stems from the conditional statement,

$$\lambda_1[\mathbf{A}_a : \mathbf{E}] = \begin{cases} \lambda_{-1}, & \mathbf{A}_a : \mathbf{E} < 0, \\ \lambda_{+1}, & \mathbf{A}_a : \mathbf{E} > 0. \end{cases} \quad (10)$$

This signifies that the material properties λ_1 differ whether the normal strain component along the direction \mathbf{a}_a is compressive or tensile.

From classical physical chemistry, the chemical potential (or more generally, the electrochemical potential) of inviscid water is given by

$$\tilde{\mu}^w = \tilde{\mu}_o^w + \frac{1}{\rho_T^w} \left[p - RT \sum_{\alpha=+,-} (\Phi_\alpha c_\alpha) + B_w \text{tr} \mathbf{E} \right], \quad (11)$$

where R is the ideal gas constant, T is the absolute temperature, μ_o^w is the reference chemical potential, Φ_α are the osmotic coefficients, and B_w is the coupling coefficient with the solid phase representing colligative effects stemming from the presence of the solid phase in the water. Similarly, the ion electrochemical potentials are given by

$$\tilde{\mu}^\alpha = \mu_o^\alpha + \left(\frac{RT}{M_\alpha} \right) \ln(\gamma_\alpha c_\alpha) + z_\alpha \frac{F_c \psi}{M_\alpha}, \quad (12)$$

($\alpha = +, -$) where μ_o^α are the reference chemical potentials, γ_α are the activity coefficients, and ψ is the electric potential.

2.3. FRICTION MODEL FORMULATION

The most critical aspect in the formulation of a friction model in the framework of the triphasic theory is to employ quantities which are continuous across the interface of contacting articular layers. In the triphasic theory, the following boundary conditions apply:

$$[[\boldsymbol{\sigma}]] \mathbf{n} = \mathbf{0}, \quad [[\tilde{\mu}^\alpha]] = 0. \quad (13)$$

($\alpha = w, +, -$), where $[[.]]$ denotes the difference, across a boundary interface, of the enclosed quantity, and \mathbf{n} denotes the unit normal at any point on this boundary interface. A proof of the general validity of these equations for the typical conditions encountered in articular cartilage is provided in Appendix A. If the interface occurs with only an external bathing solution, these equations reduce to

$$\boldsymbol{\sigma} \mathbf{n} = -p^* \mathbf{n}, \quad \tilde{\mu}^\alpha = \tilde{\mu}^{\alpha*}, \quad (14)$$

where the superscripted asterisk denotes the corresponding quantities for the bathing solution (e.g. p^* denotes the ambient pressure). Note from Equations (8) and (14)

that neither p nor the elastic traction $\boldsymbol{\sigma}^e \mathbf{n}$ are continuous across the interface, unlike for the biphasic theory. Therefore, the friction model cannot employ these quantities as was done previously in the biphasic framework (Ateshian *et al.*, 1998), for the purpose of examining the interstitial fluid pressure contribution relative to the total contact load. To extend the concept of fluid load support originally formulated in our earlier studies (e.g. Ateshian and Wang, 1995) to the triphasic theory, we propose to define an expression for fluid pressure which represents what would be measured by a fluid pressure transducer either placed against the cartilage surface (e.g. Soltz and Ateshian, 1998) or inserted within the tissue (e.g. using a needle). (This argument is presented only to provide a physical interpretation for the mathematical formulation of fluid load support which follows.) It is assumed that this hypothetical transducer has a chamber of infinitesimal volume, filled with the same solvent and ion species as the cartilage mixture, but with no solid matrix nor fixed charges. Because of its infinitesimal dimension, all variables are taken to be homogeneous within this chamber. Satisfying the balance of water chemical potential and ion electrochemical potential between cartilage and this hypothetical chamber fluid, as given in Equation (14), and recognizing that $[[\mu_o^\alpha]] = 0$ ($\alpha = w, +, -$) and $[[\rho_T^w]] = 0$, produces the following relations at the interface of the transducer and the cartilage,

$$\tilde{p} - RT(\tilde{\Phi}_+ + \tilde{\Phi}_-)\tilde{c} = p - RT(\Phi_{+c_+} + \Phi_{-c_-}) + B_w tr \mathbf{E}, \quad (15)$$

$$\tilde{\gamma}_\pm \tilde{c} = \gamma_\pm \sqrt{c_+ c_-}, \quad (16)$$

where $\tilde{\gamma}_\pm = \sqrt{\tilde{\gamma}_+ \tilde{\gamma}_-}$, $\gamma_\pm = \sqrt{\gamma_+ \gamma_-}$, and tildes denote quantities within the pressure transducer (with $\tilde{c}_+ = \tilde{c}_- \equiv \tilde{c}$). From these relations, it is thus possible to derive a general expression for pressure of the form,

$$\begin{aligned} \tilde{p} = p - RT \left[\Phi_{+c_+} + \Phi_{-c_-} - (\tilde{\Phi}_+ + \tilde{\Phi}_-) \left(\frac{\gamma_\pm}{\tilde{\gamma}_\pm} \right) \sqrt{c_+ c_-} \right] + \\ + B_w tr \mathbf{E}, \end{aligned} \quad (17)$$

which can be interpreted to represent the directly measurable fluid pressure, anywhere within the tissue or on its boundary, including at the contact interface of two cartilage layers. We now note that Equation (17) can be posed irrespective of the presence of a pressure transducer, where the osmotic and activity coefficients, $\tilde{\Phi}_\alpha$ and $\tilde{\gamma}_\alpha$, correspond to those of a solution of the same ion species as the articular cartilage, at a concentration \tilde{c} given by Equation (16). Substituting \tilde{p} into Equation (13), it can be verified that $[[\tilde{p}]] = 0$, that is, the expression of Equation (17) is continuous across any interface. If the following stress tensor is also defined:

$$\begin{aligned} \tilde{\boldsymbol{\sigma}}^e = \boldsymbol{\sigma}^e - \left\{ RT \left[\Phi_{+c_+} + \Phi_{-c_-} - \right. \right. \\ \left. \left. - (\tilde{\Phi}_+ + \tilde{\Phi}_-) \left(\frac{\gamma_\pm}{\tilde{\gamma}_\pm} \right) \sqrt{c_+ c_-} \right] - B_w tr \mathbf{E} \right\} \mathbf{I}, \end{aligned} \quad (18)$$

then $\boldsymbol{\sigma} = -p\mathbf{I} + \boldsymbol{\sigma}^e = -\tilde{p}\mathbf{I} + \tilde{\boldsymbol{\sigma}}^e$ and therefore, from Equation (13)₁, $[[\tilde{\boldsymbol{\sigma}}^e]] \mathbf{n} = \mathbf{0}$.

Integrating this fluid pressure, minus the ambient pressure p^* , over a contact interface Γ produces a fluid load of

$$W^p = - \int_{\Gamma} (\tilde{p} - p^*) d\Gamma, \quad (19)$$

whereas the total normal load at the interface is

$$W = \int_{\Gamma} (\mathbf{n} \cdot \boldsymbol{\sigma} \mathbf{n} + p^*) d\Gamma, \quad (20)$$

with \mathbf{n} denoting the unit outward normal on Γ ¹. It is now proposed that when two opposing mixtures come into sliding contact, the most significant friction arises from the frictional interactions of the solid phases across the interface. Let the area fractions (which are equal to the volume fractions, Delesse, 1847) of each of the mixture components be given by $\phi^{\beta 0}$ and $\phi^{\beta 1}$ for the two opposing mixtures, respectively ($\beta = s, w, +, -$). Assuming smooth surfaces, the fraction of contact area Γ over which the opposing solid phases are in contact with each other is given by $\phi^{s0} \phi^{s1}$, therefore the area fraction over which the fluid pressure is actually supporting load is $1 - \phi^{s0} \phi^{s1}$ (Ateshian *et al.*, 1998). It follows from this argument that the true fluid load support is $(1 - \phi^{s0} \phi^{s1}) W^p$ and that the load transmitted across solid-to-solid contact at the interface is given by

$$W^{ss} = W - (1 - \phi^{s0} \phi^{s1}) W^p. \quad (21)$$

By definition, the measured (effective) friction coefficient at the contact interface is given by $\mu_{\text{eff}} = F/W$, where F is the friction force. Since most of the friction is presumed to occur at the solid-to-solid interface, the model postulates that the friction force is proportional to the solid-to-solid normal contact force, $F = \mu_{eq} W^{ss}$, where μ_{eq} is the friction coefficient achieved when fluid pressure has subsided, $W^p = 0$. It then follows that

$$\mu_{\text{eff}} = \mu_{eq} \left[1 - (1 - \phi^{s0} \phi^{s1}) \frac{W^p}{W} \right]. \quad (22)$$

This model properly reduces to Coulomb's law when $\phi^{s0} = \phi^{s1} = 1$ (i.e. for non-porous media); whereas it predicts negligible friction in the absence of a solid phase on either side of the interface ($\phi^{s0} = 0$ and/or $\phi^{s1} = 0$, and $W^p = W$ - conditions which subsume fluid film lubrication). Otherwise, since the ratio W^p/W is time-dependent under most loading conditions, this model produces a transient friction coefficient, as typically observed experimentally.

¹ In our earlier studies (Ateshian, 1997; Ateshian *et al.*, 1998), the ambient pressure was taken to be zero, that is, all pressure terms represented gauge pressures.

2.4. UNCONFINED COMPRESSION RESPONSE

The configuration of unconfined compression of a cylindrical cartilage plug is analyzed to produce solutions for the instantaneous and equilibrium responses under an applied step load, at any desired bathing solution salt concentration. The instantaneous response is expected to produce the maximum achievable value of W^p/W for unconfined compression, and thus the smallest possible friction coefficient; whereas the equilibrium response will produce μ_{eq} . These theoretical solutions will subsequently be compared to experimental results.

The advantage of analyzing the instantaneous and equilibrium configurations is that closed-form solutions can be achieved by recognizing that the strain field, ionic concentrations, and electric potential are all homogeneous under these conditions (assuming homogeneous material properties and fixed-charge density distribution, and neglecting the friction at the cartilage-loading platen interface). The first step in this analysis is to determine the tissue free-swelling equilibrium configuration at the current bathing solution concentration, c^* , relative to its hypertonic configuration (i.e. when $c^* \rightarrow \infty$). Then, solutions will be obtained for the instantaneous and equilibrium responses to an applied step load, relative to the configuration at c^* . For all three of these analyses, satisfying the boundary conditions of Equation (13) for electrochemical potential balance produces equations of the same form as Equation (16). Using this equation together with the electroneutrality condition of Equation (6) results in quadratic equations for the anion and cation concentrations, whose solutions are

$$\begin{aligned} c_- &= \frac{-c^F + \sqrt{c^{F2} + 4(\gamma_{\pm}^*/\gamma_{\pm})^2 c^{*2}}}{2}, \\ c_+ &= \frac{c^F + \sqrt{c^{F2} + 4(\gamma_{\pm}^*/\gamma_{\pm})^2 c^{*2}}}{2}. \end{aligned} \quad (23)$$

Note that these equations do not represent a complete solution since c^F is dependent on the strain according to Equation (3) and the traction boundary condition of Equation (13) has yet to be satisfied; thus the state of strain and the interstitial fluid pressure remain to be determined. For the configurations being analyzed, the shear strains are zero while the circumferential and radial normal strains are equal to one another (E_1) but may differ from the axial normal strain (E_0),

$$[\mathbf{E}] = \begin{bmatrix} E_1 & 0 & 0 \\ 0 & E_1 & 0 \\ 0 & 0 & E_0 \end{bmatrix}. \quad (24)$$

Substituting this state of strain into the constitutive model of Equation (9), the effective stress components become

$$\begin{aligned} \sigma_{rr}^e &= \sigma_{\theta\theta}^e = (H_A[E_1] + \lambda_2)E_1 + \lambda_2 E_0, \\ \sigma_{zz}^e &= H_A[E_0]E_0 + 2\lambda_2 E_1, \end{aligned} \quad (25)$$

where $H_A[\cdot] = H_{-A} = \lambda_{-1} + 2\mu$ when its argument is negative, and $H_A[\cdot] = H_{+A} = \lambda_{+1} + 2\mu$ when its argument is positive.

2.4.1. Free-Swelling

For this reference starting configuration, the remaining boundary conditions reduces to $\boldsymbol{\sigma}\mathbf{n} = -p^*\mathbf{n}$ and $\tilde{p} = p^*$ or alternatively, $\tilde{\boldsymbol{\sigma}}^e\mathbf{n} = \mathbf{0}$. Because the swelling produces tensile normal strains, $H_A[E_0^r] = H_A[E_1^r] = H_{+A}$ in Equation (25) (where the superscript r denotes the free-swelling reference state), and it follows from the isotropic chemical stress loading that $E_1^r = E_0^r$, $\sigma_{rr}^e = \sigma_{\theta\theta}^e = \sigma_{zz}^e = (H_{+A} + 2\lambda_2)E_0^r$, and $tr\mathbf{E} = 3E_0^r$. Using Equations (18) and (23) and the boundary condition $\tilde{\boldsymbol{\sigma}}^e\mathbf{n} = \mathbf{0}$ with these results,

$$E_0^r = \frac{RT}{H_{+A} + 2\lambda_2 + 3B_w} \left[(\Phi_+ - \Phi_-) \left(\frac{c^F}{2} \right) + \right. \\ \left. + (\Phi_+ + \Phi_-) \sqrt{\left(\frac{c^F}{2} \right)^2 + \left(\frac{\gamma_{\pm}^*}{\gamma_{\pm}} \right)^2 c^{*2}} - (\Phi_+^* + \Phi_-^*)c^* \right], \quad (26)$$

where

$$c^F = c_{\infty}^F \left(\frac{1 - 3E_0^r}{\phi_{\infty}^w} \right). \quad (27)$$

The quadratic system in E_0^r formed by these two equations can be solved in closed-form, with only one of the two roots corresponding to the desired solution; however, the general expression for this solution is too cumbersome to present here. A typical variation of the free-swelling strain with bathing solution salt concentration is shown in Figure 1, demonstrating that the swelling strain is greatest at $c^* = 0$ and tends to zero as $c^* \rightarrow \infty$. From Equation (17), the osmotic pressure within the tissue, minus the ambient pressure, is

$$p - p^* = RT \left[(\Phi_+ - \Phi_-) \left(\frac{c^F}{2} \right) + (\Phi_+ + \Phi_-) \sqrt{\left(\frac{c^F}{2} \right)^2 + \left(\frac{\gamma_{\pm}^*}{\gamma_{\pm}} \right)^2 c^{*2}} - \right. \\ \left. - (\Phi_+^* + \Phi_-^*)c^* \right] - B_w tr\mathbf{E}, \quad (28)$$

and a typical dependence of this expression on c^* is presented in Figure 2. These findings are in agreement with the longstanding understanding of cartilage swelling, as reviewed for example by Maroudas (1968, 1979). At the lowest salt concentrations c^* of the external bathing solution, the electrostatic forces generated in the negatively charged proteoglycans and the influx of water and ions into the cartilage

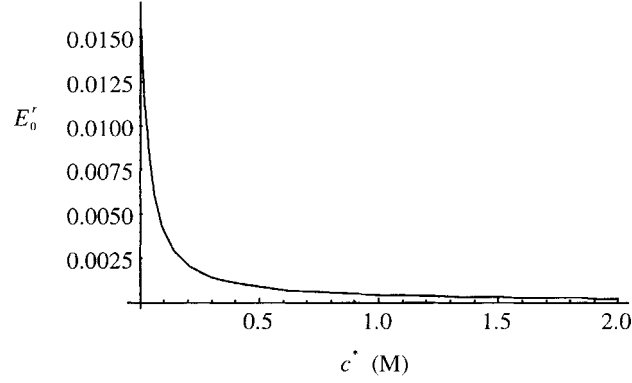


Figure 1. Free-swelling strain, E_0^r , as a function of bathing solution salt concentration, c^* , for typical material constants ($H_{-A} = 0.6$ MPa, $H_{+A} = 13.2$ MPa, $\lambda_2 = 0.48$ MPa, $B_w = 0$, $\gamma_{\pm}/\gamma_{\pm}^* = 1$, $\Phi_+ = \Phi_- = \Phi_+^* = \Phi_-^* = 1$, $c_{\infty}^F = 100$ Eq/m³, $\phi_{\infty}^w = 0.8$), and at $T = 300$ K.

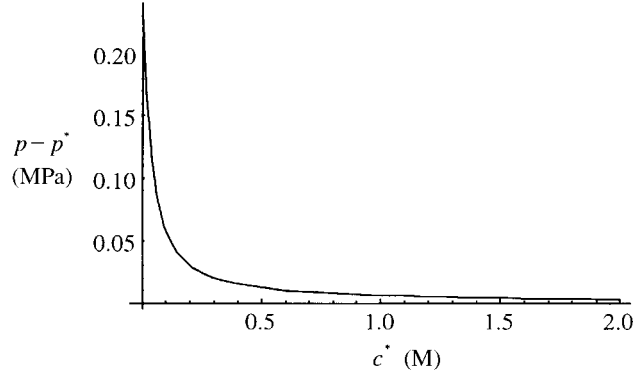


Figure 2. Osmotic pressure, $p - p^*$, under free-swelling, as a function of bathing solution salt concentration, c^* (same properties as in Figure 1).

cause the greatest amount of swelling, stretching the collagen-proteoglycan matrix until the strain in the matrix is balanced by the swelling pressure of the interstitial fluid. At the higher values of c^* , the electrostatic forces become negligible and only entropic effects remain, leading to a reduction in the swelling pressure and strain.

2.4.2. Equilibrium Response to an Applied Axial Strain

Starting from the reference free-swelling configuration described above, let an incremental axial normal strain ΔE_0 be applied, such that the total axial strain is now $E_0 = E_0^r + \Delta E_0$. The radial and circumferential strains can then be represented by $E_1 = E_0^r + \Delta E_1$, where ΔE_1 remains to be determined, and the tissue dilatation is equal to $tr\mathbf{E} = E_0 + 2E_1 = 3E_0^r + \Delta E_0 + 2\Delta E_1$. For the case where $E_0 < 0$ (and thus typically $E_1 > 0$), the normal radial and axial effective stress components are given by

$$\begin{aligned}\sigma_{rr}^e &= (H_{+A} + 2\lambda_2)E_0^r + \lambda_2\Delta E_0 + (H_{+A} + \lambda_2)\Delta E_1, \\ \sigma_{zz}^e &= (H_{-A} + 2\lambda_2)E_0^r + H_{-A}\Delta E_0 + 2\lambda_2\Delta E_1,\end{aligned}\quad (29)$$

and the boundary conditions require that $\sigma_{rr} = -\tilde{p} + \tilde{\sigma}_{rr}^e = -p^*$ and $\tilde{p} = p^*$ (or equivalently, $\tilde{\sigma}_{rr}^e = 0$) on the lateral boundary of the cylindrical specimen, while $\sigma_{zz} = -\tilde{p} + \tilde{\sigma}_{zz}^e = -p^* + \sigma_a$ (or equivalently, $\tilde{\sigma}_{zz}^e = \sigma_a$) at the top and bottom surfaces, where σ_a is the applied stress (above the ambient pressure p^*). These boundary conditions, together with Equations (18) and (29), produce the following system of equations,

$$\begin{aligned}&(H_{+A} + 2\lambda_2 + 3B_w)E_0^r + (\lambda_2 + B_w)\Delta E_0 + (H_{+A} + \lambda_2 + 2B_w)\Delta E_1 \\ &= RT \left[(\Phi_+ - \Phi_-) \left(\frac{c^F}{2} \right) + \right. \\ &\quad \left. + (\Phi_+ + \Phi_-) \sqrt{\left(\frac{c^F}{2} \right)^2 + \left(\frac{\gamma_{\pm}^*}{\gamma_{\pm}} \right)^2 c^{*2}} - (\Phi_+^* + \Phi_-^*)c^* \right],\end{aligned}\quad (30)$$

$$\sigma_a = (H_{-A} - H_{+A})E_0^r + (H_{-A} - \lambda_2)\Delta E_0 + (\lambda_2 - H_{+A})\Delta E_1,\quad (31)$$

$$c^F = c_{\infty}^F \left[1 - \frac{(3E_0^r + \Delta E_0 + 2\Delta E_1)}{\phi_{\infty}^w} \right].\quad (32)$$

Substituting Equation (32) into Equations (30), (31) produces two equations which can be solved in closed-form for the unknowns ΔE_1 and the applied stress σ_a , given ΔE_0 and reference free-swelling strain E_0^r . (The general expression for the solution is again too cumbersome to present here.) The osmotic pressure is given by the same expression as in Equation (28), however, using Equation (32) for c^F . A representative variation of this pressure with applied strain ΔE_0 and concentration c^* is shown in Figure 3. Note that an apparent equilibrium compressive Young's modulus can be derived from this solution, $E_{-Y}^{\text{app}} = \partial\sigma_a/\partial\Delta E_0$, which is dependent on the free-swelling reference configuration (Figure 4). From the above results and Equation (19), it is clear that $W^p = 0$ at this equilibrium configuration; hence, if one of the loading platens is sliding against the cartilage, the frictional model of Equation (22) would predict $\mu_{\text{eff}} = \mu_{\text{eq}}$ as expected.

2.4.3. Instantaneous Response to an Applied Axial Strain

The solution for the instantaneous response can be achieved by recognizing that the incremental solid matrix deformation must be isochoric under sudden loading (Mak *et al.*, 1987; Ateshian *et al.*, 1994). In this case, $\text{tr}\mathbf{E} = E_0 + 2E_1 = 3E_0^r +$

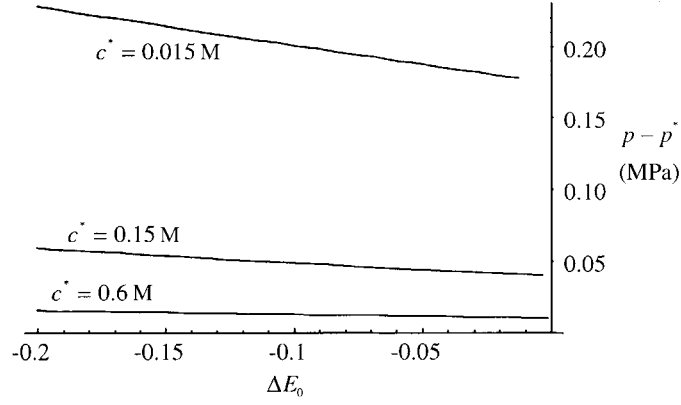


Figure 3. Equilibrium osmotic pressure minus ambient pressure, $p - p^*$, as a function of applied compressive axial strain ΔE_0 , at three representative values of c^* (same properties as in Figure 1).

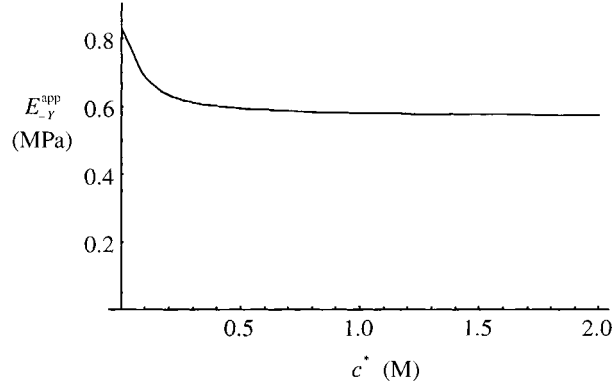


Figure 4. Apparent equilibrium compressive modulus, E_{-Y}^{app} , as a function of bathing solution salt concentration, c^* , evaluated at an axial normal strain $E_0 = E_0^r + \Delta E_0 = 0$ (i.e. when $\Delta E_0 = -E_0^r$ where the reference strain varies with c^* as shown in Figure 1).

$\Delta E_0 + 2\Delta E_1 = 3E_0^r$ (i.e. $\Delta E_0 + 2\Delta E_1 = 0$). The boundary conditions for this case are $\sigma_{rr} = -\tilde{p} + \tilde{\sigma}_{rr}^e = -p^*$ and $\sigma_{zz} = -\tilde{p} + \tilde{\sigma}_{zz}^e = -p^* + \sigma_a$, or

$$\begin{aligned} \tilde{p} = & p^* + (H_{+A} + 2\lambda_2 + 3B_w)E_0^r + (\lambda_2 - H_{+A})\left(\frac{\Delta E_0}{2}\right) - \\ & - RT \left[(\Phi_+ - \Phi_-)\left(\frac{c^F}{2}\right) + \right. \\ & \left. + (\Phi_+ + \Phi_-)\sqrt{\left(\frac{c^F}{2}\right)^2 + \left(\frac{\gamma_{\pm}^*}{\gamma_{\pm}}\right)^2 c^{*2}} - (\Phi_+^* + \Phi_-^*)c^* \right], \end{aligned} \quad (33)$$

$$\sigma_a = (H_{-A} - H_{+A})E_0^r + \left(H_{-A} - \frac{3\lambda_2}{2} + \frac{H_{+A}}{2} \right) \Delta E_0, \quad (34)$$

$$c^F = c_\infty^F \left(1 - \frac{3E_0^r}{\phi_\infty^w} \right). \quad (35)$$

Equation (34) can be solved for ΔE_0 given σ_a and E_0^r . In addition, it should be noted that since Equation (35) is identical with Equation (27), substituting Equation (26) into Equation (33) produces

$$\tilde{p} = p^* + (\lambda_2 - H_{+A}) \left(\frac{\Delta E_0}{2} \right), \quad (36)$$

and the instantaneous fluid load support would then be

$$\frac{W^P}{W} = \frac{H_{+A} - \lambda_2}{2H_{-A} - 3\lambda_2 + H_{+A} - 2(H_{+A} - H_{-A})E_0^r/\Delta E_0}. \quad (37)$$

It can be noted from this equation and the representative response in Figure 5 that the fluid load support is dependent on the reference configuration at the bathing concentration of c^* , as well as the applied compressive strain ΔE_0 ; in particular, if $E_0 = E_0^r + \Delta E_0 = 0$, then $W^P/W = 1/3$ (and if $E_0 > 0$, all instances of H_{-A} would be replaced with H_{+A} in Equation (37), also producing $W^P/W = 1/3$). An instantaneous apparent compressive modulus can also be derived from the above solution, $E_{-I}^{\text{app}} = \partial\sigma_a/\partial\Delta E_0 = H_{-A} - 3\lambda_2/2 + H_{+A}/2$, which is independent of the free-swelling configuration.

According to Equation (22), the effective friction coefficient, μ_{eff} , achieves its smallest value (denoted by μ_{min}) when W^P/W is greatest; for the current analysis, this occurs at the instantaneous response. Thus, a prediction of μ_{min} , or $\mu_{\text{min}}/\mu_{\text{eq}}$, can be achieved by substituting the result of Equation (37) into Equation (22); using

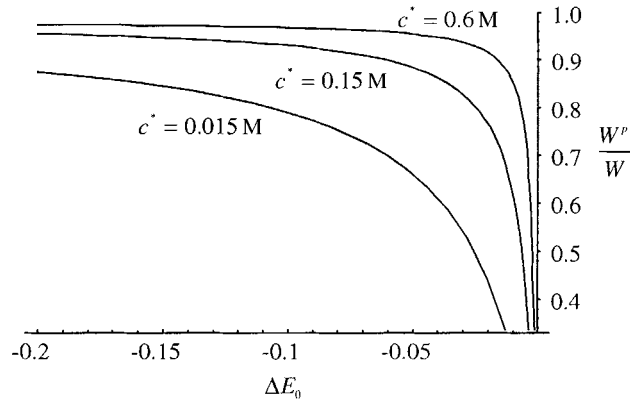


Figure 5. Instantaneous fluid load support, W^P/W , as a function of applied compressive axial strain ΔE_0 , at three representative values of c^* (same properties as in Figure 1).

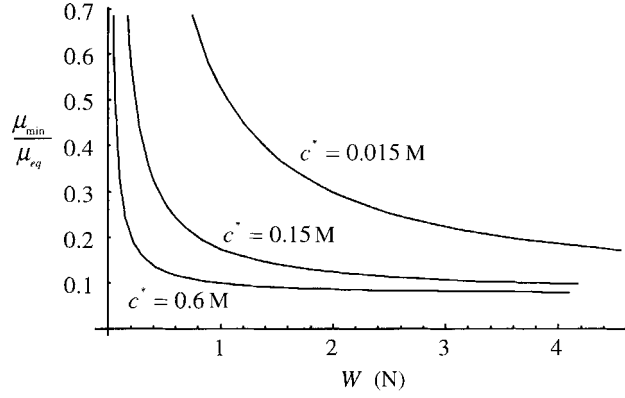


Figure 6. The ratio μ_{\min}/μ_{eq} as predicted from Equation (22) when using the instantaneous fluid load support as given in Equation (37), as a function of c^* and $W = -\sigma_a(\pi r_0^2)$ (where σ_a is given in Eq. (34)), assuming a cylindrical sample of radius $r_0 = 1$ mm; $\phi^{s0}\phi^{s1} = 0.05$, other properties as in Figure 1.

a representative value of $\phi^{s0}\phi^{s1} = 0.05$, the dependence of μ_{\min}/μ_{eq} on load and bathing solution concentration is presented in Figure 6.

2.4.4. Transient Response

A complete analysis of the transient response in unconfined compression can be achieved numerically. Please see the study by Sun *et al.* (1999) for a formulation of the governing mixture theory equations suitable for a finite element or finite difference analysis. In addition to the material properties employed in the instantaneous and equilibrium responses above, a transient analysis also requires that the following properties be provided: $k = \phi^{w^2}/f_{ws}$ (the hydraulic permeability of the porous solid matrix), $D^+ = RT\phi^w c_+/f_{+w}$ (the diffusion coefficient for the cation), and $D^- = RT\phi^w c_-/f_{-w}$ (the diffusion coefficient for the anion); all three of these properties are taken to be constant here. All other frictional coefficients in Equation (4) are assumed negligible ($f_{s+} = f_{s-} = f_{+-} = 0$). For the current problem, the transient response was achieved under a step load (creep response), in analogy to the analysis above and the experiments described below. All the dependent variables of this problem can be obtained from the numerical solution, though only select responses are provided here. The ratios W^p/W and $\mu_{\text{eff}}/\mu_{eq}$, evaluated from Equations (17)–(22), are presented in Figure 7 for a typical applied load and bathing solution salt concentration. These responses predict a monotonic increase in the effective friction coefficient, for a given equilibrium friction coefficient, with the minimum friction coefficient occurring at $t = 0^+$ as expected.

3. Experimental Methods and Results

Experiments were conducted to investigate the trends suggested by the theoretical analysis above. However, it should be noted that the experiments described

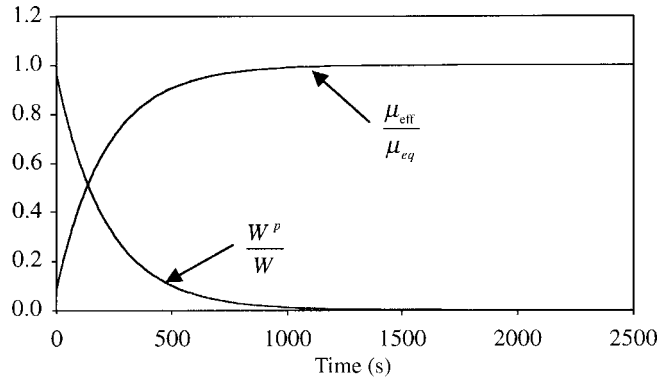


Figure 7. Typical transient response of W^P/W and μ_{eff}/μ_{eq} obtained from a finite difference solution of the governing equations for unconfined compression creep under an applied load of $W = 0.5$ N and with $c^* = 0.6$ M. ($H_{-A} = 0.6$ MPa, $H_{+A} = 13.2$ MPa, $\lambda_2 = 0.48$ MPa, $B_w = 0$, $\gamma_{\pm}/\gamma_{\pm}^* = 1$, $\Phi_+ = \Phi_- = \Phi_+^* = \Phi_-^* = 1$, $c_{\infty}^F = 20$ Eq/m³, $\phi_{\infty}^w = 0.8$, $T = 300$ K, $k = 1.0 \times 10^{-15}$ m⁴/N.s, $D^+ = 0.5 \times 10^{-9}$ m²/s², $D^- = 0.8 \times 10^{-9}$ m²/s², $\phi^{s0}\phi^{s1} = 0.05$.)

here achieved strains in the finite deformation range, hence comparisons with the theoretical analysis are only intended to be qualitative. Six cylindrical cartilage plugs (diam. = 4.78 mm) were harvested from shoulder joints of freshly sacrificed 6–10-month-old cows. From each of these disks, three plugs were cored (diam. = 2.0 mm) and stored in different concentrations of PBS solution (0.6, 0.15, and 0.015 M). At the time of testing, each sample was thawed, its thickness measured, and placed into a custom friction device (Figure 8) with the articular surface facing

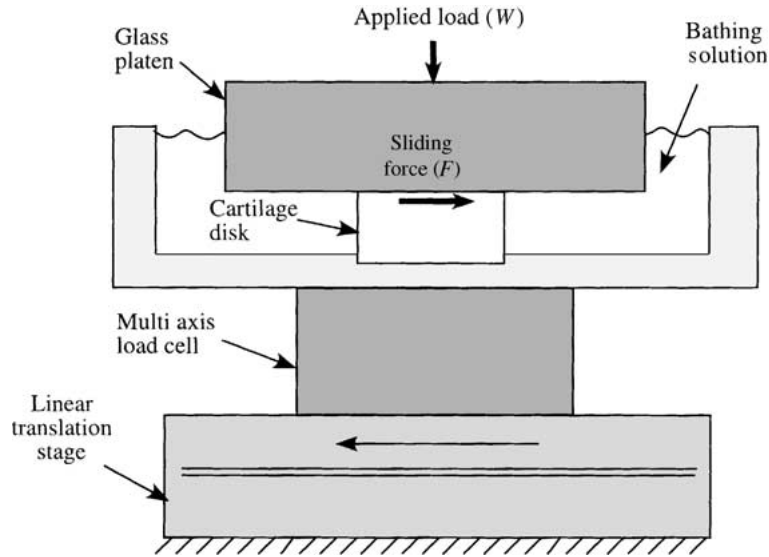


Figure 8. Schematic of the experimental configuration.

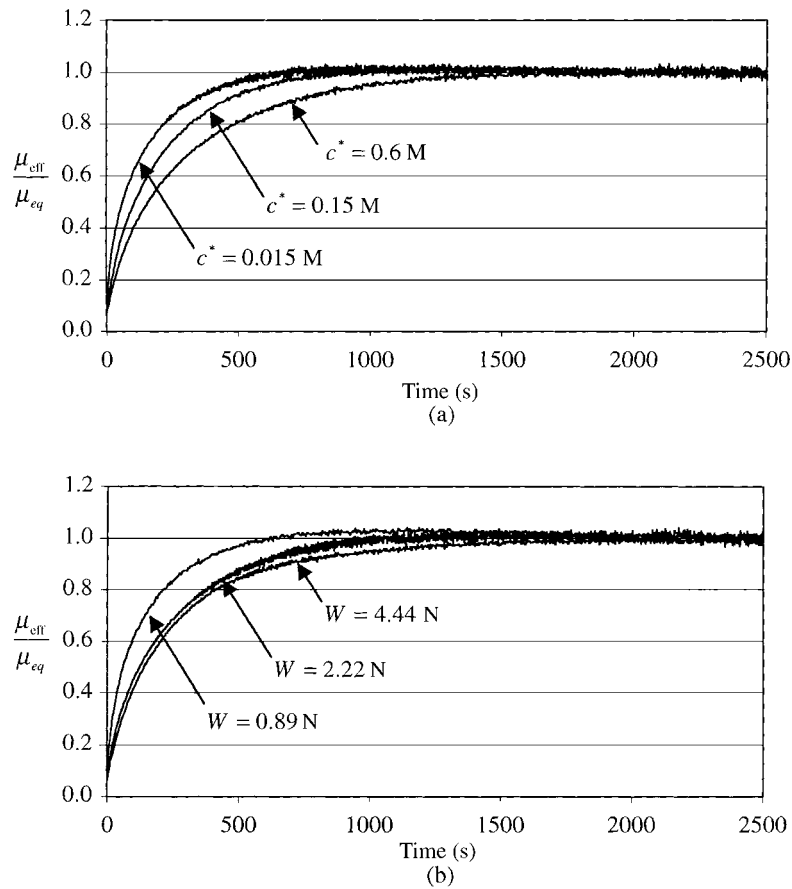


Figure 9. Average experimental frictional response of $\mu_{\text{eff}}/\mu_{\text{eq}}$ versus time, as a function of (a) bathing solution concentration c^* (for all loads), and (b) applied load W (for all concentrations). Each curve represents the average of 18 tests.

a smooth glass platen. Without applying an initial tare load, the glass platen was lowered onto the surface of the tissue at a rate of $10 \mu\text{m/s}$ until a constant load of either 0.89, 2.22, or 4.45 N was achieved²; this constant load was maintained by feedback control until equilibrium was reached ($\sim 2500 \text{ s}$). Simultaneously, a reciprocal sliding motion was produced with a linear translation stage (Model PM500-1L, Newport Corp., Irvine CA) between the sample and glass platen, at a constant velocity of 1 mm/s , spanning 4 mm in each direction. The normal applied load (W) and frictional sliding force (F) were measured with a multi-axis load cell (JR3, Woodland CA), and the creep deformation with an LVDT (Macro Sensors, NJ). The time-dependent friction coefficient ($\mu_{\text{eff}} = F/W$) was evaluated from the force measurements (Figure 9). Its minimum value (μ_{min}), achieved when the

² In all cases, it took less than 30 s to achieve the desired load. Given that the time constant for flow-dependent creep and stress-relaxation is on the order of several hundred seconds, this protocol is reasonably representative of instantaneous loading.

applied load reached its desired level (<30 s), and its terminal equilibrium value (μ_{eq}) were employed in subsequent analyses. At the completion of a test, the specimen was unloaded and allowed to recover for 3600 s. Each specimen plug was tested at each of the three loads in random order; each of the three plugs from the same disk were tested at distinct salt concentrations, with six specimens employed for each concentration. A nonlinear stress-strain relationship, $\sigma = A[\exp(B\varepsilon) - 1]$, was fitted to the equilibrium engineering stress and strain data acquired from the three applied loads to produce a tangent unconfined compression modulus at zero strain (AB), for each of the three concentrations.

Following all loading sequences, cartilage disks were biochemically analyzed as follows: First, wet weight was measured, followed by freezing at -30°C . Disks were then lyophilized overnight and reweighed to determine water content. For determination of sulfated glycosaminoglycan (S-GAG) content, disks were digested for 16 h with papain at 60°C in 0.1 M sodium acetate (pH 5.6) containing 0.05 M EDTA and 0.01 M cysteine-HCl. S-GAG content of the digests was determined using the 1,9-dimethylmethylene blue dye-binding assay (Farndale *et al.*, 1982), as modified for microtiter plates and using absorbances of 540 and 595 nm for improved detectability (Seibel *et al.*, 1992).

A two-way ANOVA with repeated measures on load and concentration was performed on the friction coefficients and the ratio μ_{\min}/μ_{eq} . When statistical significance was observed, pairwise p -values were evaluated from least squares means using Bonferroni adjustment to determine differences in the means. A one-way analysis with repeated measures on concentration was performed for the variables of thickness, water content, GAG content, and tangent modulus.

Out of 54 tests (three tests per plug on 18 plugs), one outlier was excluded from the analysis. The effects of concentration and load on μ_{\min} , μ_{eq} , and μ_{\min}/μ_{eq} are reported in Figure 10. All three of these parameters were statistically higher at 0.015 M than at 0.15 or 0.6 M, and at 0.89 N than at 2.22 or 4.45 N ($p < 0.05$). Increasing the bathing solution concentration decreased the thickness of the samples significantly between all concentrations ($p < 0.05$) as well as decreased the water content and tangent modulus relative to the lowest concentration (Table I). However, GAG content did not change significantly with concentration.

To investigate which of the measurable parameters could best predict the observed variation in the equilibrium friction coefficient μ_{eq} , linear regression was performed against the applied load W ($r^2 = 0.197$), the bathing solution salt concentration c^* ($r^2 = 0.076$), the equilibrium axial engineering strain ($r^2 = 0.312$), the equilibrium modulus ($r^2 = 0.103$), and the GAG per wet weight ($r^2 = 0.000$). Other than GAG content, μ_{eq} was observed to decrease with increases in these variables. The highest correlation, observed with the equilibrium engineering strain, is shown in Figure 11.

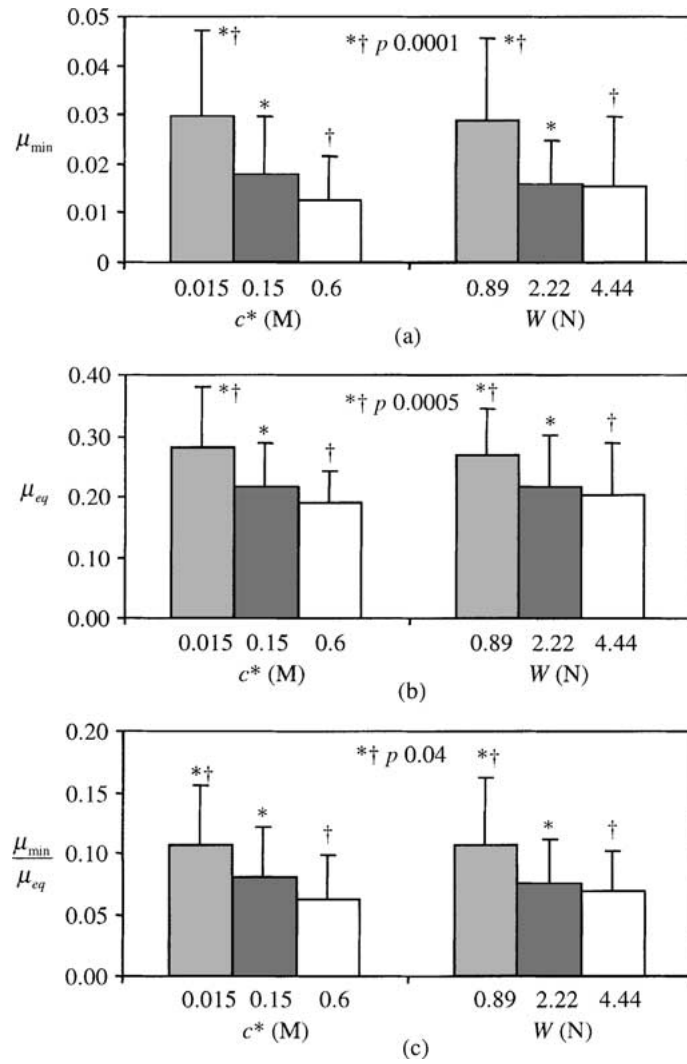


Figure 10. Average experimental results for the effect of bathing solution concentration, c^* , and load, W , on (a) μ_{\min} , (b) μ_{eq} , and (c) μ_{\min}/μ_{eq} .

Table I. Tabulation of the effect of bathing solution concentration on several measured parameters

Concentration, c^*	0.015 M	0.15 M	0.6 M
Thickness (mm)	$1.09 \pm 0.16^*$	$1.06 \pm 0.18^*$	$1.03 \pm 0.17^*$
Percentage of water content	$85.4 \pm 5.4^{*\dagger}$	$80.9 \pm 3.4^*$	$77.9 \pm 3.6^\dagger$
GAG/ $\mu\text{g}/\text{mg}$	47.4 ± 8.2	49.5 ± 14.3	44.3 ± 9.0
Tangent modulus (MPa)	$0.50 \pm 0.14^{*\dagger}$	$0.32 \pm 0.15^*$	$0.15 \pm 0.09^\dagger$

* $\dagger p < 0.05$.

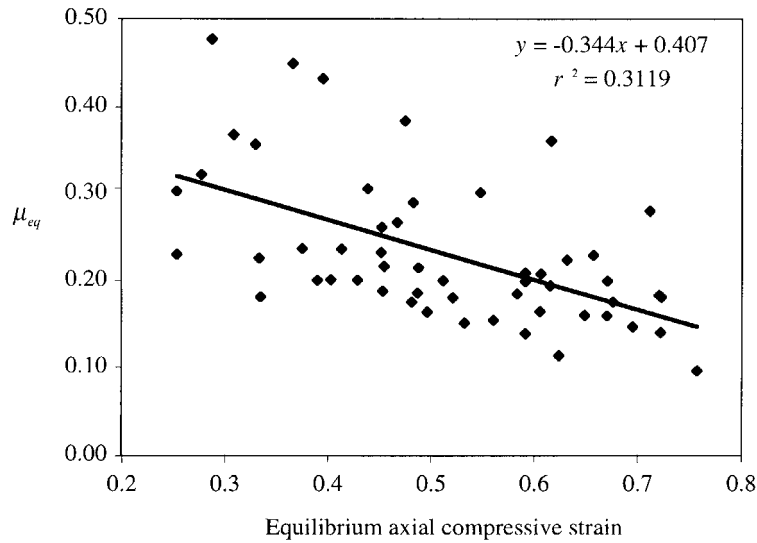


Figure 11. Correlation between experimental measurements of the equilibrium friction coefficient μ_{eq} and the equilibrium axial compressive strain.

4. Discussion

The objective of this study was to formulate a model for the frictional response of articular cartilage which accounts for osmotic effects as well as the solid matrix's tension-compression nonlinearity. The motivation for this investigation is based on the recognition that pressurization of the interstitial fluid has been proposed as a mechanism for reducing the friction coefficient of cartilage (McCutchen, 1962; Malcom, 1976; Mow *et al.*, 1980; Macirowski *et al.*, 1994; Forster and Fisher, 1996; Ateshian *et al.*, 1998), a mechanism which has been successfully modeled using biphasic constitutive relations for cartilage (Ateshian *et al.*, 1997, 1998). However, biphasic models do not directly describe the Donnan osmotic pressure which is lumped with the stiffness of the solid matrix³, therefore an analysis of this effect requires the use of mixture models incorporating electrolytes and solid matrix fixed-charge density as performed here.

The first challenge in the modeling of the frictional response of cartilage using the triphasic theory (Lai *et al.*, 1991; Gu *et al.*, 1998) was to formulate a quantity continuous across any contact interface, since frictional forces dependent on such a quantity must be equal and opposite across the interface. In addition, such formulation should reduce to the biphasic fluid pressure in the absence of fixed charges. The quantity \tilde{p} , defined by Equation (17), is such a quantity; it represents the

³ The biphasic aggregate modulus, H_A , combines the intrinsic stiffness of the solid matrix with the stiffness imparted by the osmotic pressure; whereas the triphasic moduli $H_{\pm A}$ employed here represent only the intrinsic solid matrix stiffness.

difference between the local total pressure and the local osmotic pressure against a (hypothetical) bathing solution which is in equilibrium locally with the tissue.

When two cartilage layers approach one another, it is possible that squeeze film and hydrodynamic effects may prevail for a short duration of time, whereby the surfaces are separated only by fluid (e.g. synovial fluid); however, several theoretical studies have suggested that this fluid-film lubrication mechanism is unlikely to last for more than a second or so (Hou *et al.*, 1992; Jin *et al.*, 1992; Hlavacek, 1993, 2000), and that the theoretical framework of pure fluid-film lubrication predicts friction coefficients substantially lower than observed experimentally (Dowson and Jin, 1986). Consequently, in view of the experimental finding that a low cartilage friction coefficient can be maintained for much longer durations than a second, a number of investigators have proposed that the frictional response of cartilage is in the mixed lubrication regime, where a combination of hydrodynamic and boundary lubrication prevails. The source of friction in pure fluid-film lubrication arises exclusively from the viscosity of the lubricant; whereas the friction in pure boundary lubrication is dependent upon the properties of the boundary lubricant present at the bearing surfaces, and the solid-to-solid interactions; hence, in mixed lubrication, the friction force is presumed to result from a combination of these effects. The question that has intrigued investigators over the last several decades is the nature of the role of the interstitial water within cartilage. Does this water influence the frictional response, and if so, in what ways. Hou *et al.* (1992) demonstrated that during squeeze-film lubrication of a biphasic articular layer, the pressure in the fluid-film lubricant is the same as that within the interstitial fluid of cartilage near the articular surface; Ateshian *et al.* (1994) subsequently indicated that this interstitial fluid pressure remains essentially unchanged for hundreds of seconds if contact occurs in the absence of a fluid-film lubricant ('boundary contact'), suggesting that there can be a total depletion of the fluid-film after a few seconds of squeeze-film action and yet no loss of pressurization within the interstitial water of cartilage for much longer durations. Furthermore, in a rolling and sliding boundary contact study (Ateshian and Wang, 1995), it was demonstrated that a very elevated hydrostatic pressurization of interstitial fluid can be maintained under steady-state rolling and sliding despite the absence of a fluid-film lubricant. Hou *et al.* (1992), Jin *et al.* (1992), and Hlavacek (2000) demonstrated that squeeze-film action is in fact defeated by the porous nature of cartilage, when compared to impermeable bearing surfaces, because the pores present an additional pathway for the squeeze-film lubricant to escape the high-pressure regions. Therefore, the theoretical evidence strongly suggests that pure fluid-film lubrication cannot be sustained for more than a few seconds at best, but that the interstitial water of cartilage can nevertheless remain pressurized for much longer times; during the short transition from fluid-film lubrication to boundary contact, the interstitial fluid pressure *within* cartilage is the same as in the fluid film, and decreases only very slowly over several hundred seconds following fluid-film depletion. The friction model proposed in this study represents a mathematical formulation, within the framework of mixture theory,

of hypotheses that have been proposed previously in the literature which explain the role of the interstitial water in the frictional response. Under this hypothesis, the hydrostatic pressurization of the interstitial fluid contributes significantly to the load W supported across the contact interface, even in the absence of a fluid film lubricant separating the articular surfaces. The load supported by the interstitial fluid depends on the fraction of the contact area over which solid-to-solid contact occurs; if the articular surfaces are perfectly smooth and in the absence of a thin film lubricant, the solid-to-solid contact area fraction is given by $\phi = \phi^{s0}\phi^{s1}$; if the surfaces are not in direct contact, that is, in the presence of a thin film lubricant, the solid-to-solid contact area fraction is simply $\phi = 0$; and if the surfaces are only in partial contact (e.g. if the surfaces are not smooth) then $0 \leq \phi \leq \phi^{s0}\phi^{s1}$. Accordingly, the load supported by the fluid is given by $(1 - \phi)W^p$ and it can be easily verified that this expression spans the range from fluid-film to boundary contact, including in the limit when the bearing surfaces are non-porous. Based on the theoretical evidence from the literature, which shows that the predicted friction coefficient from hydrodynamic lubrication theory is two orders of magnitude smaller than the observed minimum friction coefficient of cartilage, we hypothesized in the current model that the friction force arising from the viscosity of the interstitial water of cartilage and/or the viscosity of the synovial fluid is negligible, and that the major contribution to the observed friction coefficient arises from the solid-to-solid interactions. Hence, the friction force is taken to be proportional to W^{ss} in Equation (21), or more generally $W^{ss} = W - (1 - \phi)W^p$. This should not be misconstrued to mean that interstitial water plays no role in the frictional response of cartilage; on the contrary, the primary role of the interstitial water is to reduce the magnitude of the load, and hence the friction force, transmitted across solid-to-solid interactions as indicated in Equation (22).

The most evident finding of this study is that the observed transient response of the friction coefficient, as represented by $\mu_{\text{eff}}/\mu_{\text{eq}}$ in Figure 9, can be predicted by the proposed model as shown in Figure 7. Indeed, it is possible to reproduce from theory a time-varying response with a very similar time constant as the experimental results, on the order of a few hundred seconds. From purely experimental considerations, the magnitude of this time constant strongly suggests that squeeze-film lubrication effects cannot account alone for the observed response, since squeeze-film times for a water-based saline solution simply could not exceed a few seconds at best. Consequently, in view of the agreement observed with the theoretically predicted transient response, the premise of the proposed friction model appears to be supported, namely that the frictional force results primarily from solid-to-solid interactions at the contact interface. The model postulates that these interactions are dependent on the magnitude of interstitial fluid pressurization within the cartilage and not on the thickness of a putative fluid film. Thus, when load is applied onto cartilage, a very large fraction of it is initially supported by the fluid inside cartilage and only a small fraction is supported by the solid matrix, yielding a very small friction coefficient at early times. As the water

exudes from the tissue sideways along the radial direction, with a characteristic time constant on the order of hundreds of seconds, the interstitial fluid pressure decreases accordingly and contributes less and less to the load support which shifts increasingly to the solid phase, with a concomitant increase in the friction coefficient.

The experimental findings of this study demonstrate that the friction coefficient of cartilage can be as small as 0.013 at early loading times and as high as 0.28 after a long duration of loading (Figure 10). The low value of μ_{\min} is in good agreement with other reports in the literature and agrees with the expectation that cartilage is an excellent bearing material. Some investigators have maintained that this remarkably low friction coefficient should be attributed to a boundary lubricant present in the cartilage or synovial fluid, with lubricating glycoproteins (Swann and Radin, 1972; Swann *et al.*, 1979) and phospholipids (Hills, 1989) ranking high on the list of candidates. However, under this hypothesis, the friction coefficient would presumably remain small at all times, which is belied by the experimental findings reported here and in previous studies (McCutchen, 1962; Forster and Fisher, 1996), as attested by the relatively high values of μ_{eq} . Indeed, the ratio of μ_{\min} to μ_{eq} ranged on average from 0.06 to 0.11 in the current study (Figure 10); importantly, the increase from μ_{\min} to μ_{eq} did not represent a permanent alteration in the cartilage since allowing the tissue to recover, and repeating the frictional test on the same sample at different loads (as performed in this study), demonstrated that the large reduction in the friction coefficient at early times was highly repeatable. As opposed to the alternative hypotheses of hydrodynamic fluid film lubrication and pure boundary lubrication, the mechanism proposed in this study is able to account for the observed ratio μ_{\min}/μ_{eq} as can be noted in Figures 6 and 10, because a dramatic change occurs in the percentage of fluid load support W^p/W over the duration of the test, where it decreases from a typical value of 97% at early times down to 0% at equilibrium.

Unlike the predictions for μ_{\min} and μ_{\min}/μ_{eq} , the current model does not predicate a particular response for the equilibrium friction coefficient, μ_{eq} . In other words, whether μ_{eq} remains constant or varies under certain conditions does not enter directly into the hypothesis that fluid load support is responsible for the time-dependent response of the friction coefficient. Based on the work of Unsworth *et al.* (1975), Malcom (1976), Swann *et al.* (1979), Hills (1989) and others, we had previously speculated that μ_{eq} could depend on the sliding velocity, the applied load, the surface roughness, or the presence of a boundary lubricant at the articular surfaces (Ateshian, 1997; Ateshian *et al.*, 1998). Of the factors investigated in the current study, it was observed that μ_{eq} correlated best with the magnitude of the axial compressive strain under equilibrium conditions (Figure 11), a finding consistent with one of our earlier studies (Wang and Ateshian, 1997); clearly, from Figure 10(b), μ_{eq} also varied with load and concentration, but the correlation analysis suggests that the axial strain, which also depends on applied load and concentration, has a more direct influence on the equilibrium friction coefficient. At this time we can

only speculate on why this dependence occurs, for example, as a result of flattening of surface roughness or factors affecting the molecular forces of macromolecules present at the articular surface, including electrostatic forces.

In addition to these findings on μ_{eff} and $\mu_{\text{min}}/\mu_{\text{eq}}$, experimental measurements of the thickness, water content, and unconfined compression modulus of cartilage as a function of bathing solution concentration and applied load are found to be in qualitative agreement with the predictions of the triphasic solution presented here. Indeed, the decreasing thickness of cartilage observed with increasing c^* (Table I) is consistent with the behavior of the free-swelling strain, E_0^r , as shown in Figure 1; similarly with the decreasing water content, ϕ^w (Table I) as predicated by Equation (2). The decrease in equilibrium unconfined compression modulus with increasing c^* (Table I) is similarly consistent with the trend calculated for E_{-Y}^{app} in Figure 4, whereas the increase in modulus with greater applied loads is partly due to the increase in osmotic pressure with compressive strain, as shown in Figure 3. Consequently, at least from these qualitative agreements, it is reasonable to conclude that the theoretical framework of the triphasic theory is able to explain these observed phenomena. Hence, even though cartilage Donnan osmotic pressure could not be measured directly, its response may be inferred from the indirect measurements presented here, namely, that osmotic pressure increases with decreasing bathing solution concentration, and increases with increasing applied load.

It is interesting to note that $\mu_{\text{min}}/\mu_{\text{eq}}$ is observed to follow opposite trends when increasing osmotic pressure by these two alternate mechanisms. With concentration-induced increases in osmotic pressure $\mu_{\text{min}}/\mu_{\text{eq}}$ increased, but with load-induced increases in osmotic pressure this ratio decreased (Figure 10(c)). From theory, the results of Figure 5 indicate that the instantaneous (maximum) fluid load support W^p/W increases with increasing salt concentration (i.e. decreasing osmotic pressure, Figure 2) and with increasing compressive strain or load (i.e. increasing osmotic pressure, Figure 3). This higher fluid load support produces a ratio $\mu_{\text{min}}/\mu_{\text{eq}}$ which decreases with increasing c^* and increasing W , as demonstrated from theory in Figure 6 and verified experimentally in Figure 10(c). When the tissue is initially in a free-swelling state, the strain field is isotropic with all three normal components being in tension and given by E_0^r ; thus, near the free-swelling state, the stress-strain response is linear since there is no mixing of tensile and compressive normal strain components. As is also the case for a biphasic material (Armstrong *et al.*, 1984), so long as the total applied axial strain $E_0^r + \Delta E_0$ is positive, the instantaneous fluid load support is 1/3 of the total applied load according to Equation (37) and will remain at this value until $E_0^r + \Delta E_0$ becomes negative (Figure 5). The smaller the value of c^* , the greater the magnitude of ΔE_0 required to overcome the swelling strain so as to make the axial strain compressive; however, when $|\Delta E_0/E_0^r| \gg 1$, the effect of this initial swelling becomes negligible and the fluid load support becomes comparable to the case of a biphasic-CLE model where swelling effects are neglected (Soltz and Ateshian, 2000b). Thus, the

tension-compression nonlinearity of cartilage plays a crucial role in modulating the interstitial fluid pressurization and consequently the transient response of the friction coefficient of cartilage.

Finally, it is important to comment on the question as to how can cartilage be considered a good bearing material if its friction coefficient remains small only for a few hundred seconds but then reaches the relatively high value of 0.28 under equilibrium conditions. The answer to this question is that interstitial fluid load support never drops to zero and always remains very substantial under physiological loading conditions, because human joints always experience some form of intermittent loading. There is no physiological circumstance of normal daily activities where a load can be applied across cartilage and maintained perfectly static for thousands of seconds, as is possible in laboratory testing conditions. In our previous study (Ateshian, 1997), we provided evidence from the literature that any motion of the joints, even if sliding at speeds as low as 0.1 mm/s, will produce and sustain a high interstitial fluid load support. Our experimental measurements of interstitial fluid pressurization (Soltz and Ateshian, 1998, 2000a) demonstrate that intermittent loading at frequencies as low as 10^{-4} Hz will still pressurize cartilage considerably, and it is safe to assume that the characteristic frequency of joint loading (even in the upper extremities) is more likely to be in the range of 10^{-3} – 10^0 Hz. Consequently, under physiological conditions, the friction coefficient of cartilage remains much closer to 0.013 (the lower range of our measurements) than 0.28 (the upper range of our measurements).

The results of this study advance our understanding of the mechanism of lubrication in diarthrodial joints, whose primary function is to transmit joint loads with low friction and wear. This study presents a new formulation of our previously described friction model for cartilage, within the framework of the triphasic theory for soft hydrated charged tissues and the conewise linear elasticity theory for bimodular materials. This formulation is able to describe the time-dependent response of the friction coefficient of articular cartilage, as well as its dependence on applied load and bathing solution salt concentration. This study also clarifies the role of osmotic effects in the interstitial fluid pressurization load support mechanism of articular cartilage.

Appendix A: Interface Jump Conditions

In this Appendix the interface jump conditions are derived and the assumptions employed in the current analysis are detailed. The balance of mass, linear momentum, and energy, and the entropy inequality for a mixture of multiple phases are given by

$$\sum_{\alpha} \frac{d}{dt} \int_R \rho^{\alpha} dV + \int_{\partial R} \rho^{\alpha} (\mathbf{v}^{\alpha} - \mathbf{v}_R) \cdot \mathbf{n} dS = 0, \quad (\text{A.1})$$

$$\begin{aligned}
 & \sum_{\alpha} \frac{d}{dt} \int_R \rho^{\alpha} \mathbf{v}^{\alpha} dV + \int_{\partial R} \rho^{\alpha} \mathbf{v}^{\alpha} (\mathbf{v}^{\alpha} - \mathbf{v}_R) \cdot \mathbf{n} dS \\
 & = \sum_{\alpha} \int_{\partial R} \boldsymbol{\sigma}^{\alpha} \mathbf{n} dS + \int_R \rho^{\alpha} \mathbf{b}^{\alpha} dV, \tag{A.2}
 \end{aligned}$$

$$\begin{aligned}
 & \sum_{\alpha} \frac{d}{dt} \int_R \rho^{\alpha} \left(\varepsilon^{\alpha} + \frac{1}{2} \mathbf{v}^{\alpha} \cdot \mathbf{v}^{\alpha} \right) dV \\
 & = \sum_{\alpha} \int_{\partial R} \mathbf{v}^{\alpha} \cdot \boldsymbol{\sigma}^{\alpha} \mathbf{n} dS - \int_{\partial R} \rho^{\alpha} \left(\varepsilon^{\alpha} + \frac{1}{2} \mathbf{v}^{\alpha} \cdot \mathbf{v}^{\alpha} \right) (\mathbf{v}^{\alpha} - \mathbf{v}_R) \cdot \mathbf{n} dS + \\
 & \quad + \int_R \rho^{\alpha} \mathbf{b}^{\alpha} \cdot \mathbf{v}^{\alpha} dV - \int_{\partial R} \mathbf{h}^{\alpha} \cdot \mathbf{n} dS + \int_R \rho^{\alpha} r^{\alpha} dV, \tag{A.3}
 \end{aligned}$$

$$\begin{aligned}
 & \sum_{\alpha} \frac{d}{dt} \int_R \rho^{\alpha} \eta^{\alpha} dV + \int_{\partial R} \rho^{\alpha} \eta^{\alpha} (\mathbf{v}^{\alpha} - \mathbf{v}_R) \cdot \mathbf{n} dS + \\
 & \quad + \int_{\partial R} \frac{\mathbf{h}^{\alpha}}{\theta} \cdot \mathbf{n} dS - \int_R \rho^{\alpha} \frac{r^{\alpha}}{\theta} dV \geq 0, \tag{A.4}
 \end{aligned}$$

where R is the mixture volume, \mathbf{n} is the unit outward normal to R , ρ^{α} , \mathbf{v}^{α} , $\boldsymbol{\sigma}^{\alpha}$, \mathbf{b}^{α} , ε^{α} , \mathbf{h}^{α} , r^{α} , η^{α} are the density, velocity, stress tensor, specific body force, specific internal energy, heat outflux vector, specific internal heat source, and specific entropy for the α -phase, respectively, θ is the temperature, and \mathbf{v}_R is the velocity of the boundary of the volume R .

The jump conditions for the mass, linear momentum, energy, and entropy across a discontinuous interface Γ can be derived from the above integral form of the balance equations using the Reynolds transport theorem (e.g. Hou *et al.*, 1989):

$$\left[\left[\sum_{\alpha} \rho^{\alpha} (\mathbf{v}^{\alpha} - \mathbf{v}_{\Gamma}) \right] \right] \cdot \mathbf{n} = 0, \tag{A.5}$$

$$\left[\left[\sum_{\alpha} \boldsymbol{\sigma}^{\alpha} - \rho^{\alpha} (\mathbf{v}^{\alpha} - \mathbf{v}_{\Gamma}) \otimes (\mathbf{v}^{\alpha} - \mathbf{v}_{\Gamma}) \right] \right] \cdot \mathbf{n} = \mathbf{0}, \tag{A.6}$$

$$\begin{aligned}
 & \left[\left[\sum_{\alpha} \boldsymbol{\sigma}^{\alpha T} (\mathbf{v}^{\alpha} - \mathbf{v}_{\Gamma}) - \mathbf{h}^{\alpha} - \rho^{\alpha} \right. \right. \\
 & \quad \left. \left. \left(\varepsilon^{\alpha} + \frac{1}{2} (\mathbf{v}^{\alpha} - \mathbf{v}_{\Gamma}) \cdot (\mathbf{v}^{\alpha} - \mathbf{v}_{\Gamma}) \right) (\mathbf{v}^{\alpha} - \mathbf{v}_{\Gamma}) \right] \right] \cdot \mathbf{n} = 0, \tag{A.7}
 \end{aligned}$$

$$\left[\left[\sum_{\alpha} \left(\frac{\mathbf{h}^{\alpha}}{\theta} + \rho^{\alpha} \eta^{\alpha} (\mathbf{v}^{\alpha} - \mathbf{v}_{\Gamma}) \right) \right] \right] \cdot \mathbf{n} = 0. \tag{A.8}$$

These interface jump conditions are true generally and are not limited for non-dissipative interfaces to steady-state equilibrium.

In addition, it is possible to generate jump conditions for each individual α -phase. For the present purpose, only the jump condition for the mass is provided, because it can be reduced to a special case of sufficiently general purpose:

$$[[\rho^\alpha(\mathbf{v}^\alpha - \mathbf{v}_\Gamma)]] \cdot \mathbf{n} = \delta^\alpha, \quad (\text{A.9})$$

where δ^α is the surface supply of mass to the α -phase from the remaining phases. Such mass supply terms would typically occur in chemical reactions between the phases. For hydrated biological soft tissues, however, such mass supply is typically negligible, hence it is appropriate for this general category of problems to employ the jump condition

$$[[\rho^\alpha(\mathbf{v}^\alpha - \mathbf{v}_\Gamma)]] \cdot \mathbf{n} = 0. \quad (\text{A.10})$$

The electrochemical potential of the α -phase is given by (e.g. Bowen, 1980)

$$\mathbf{K}^\alpha = \psi^\alpha \mathbf{I} - \frac{\boldsymbol{\sigma}^{\alpha T}}{\rho^\alpha}, \quad (\text{A.11})$$

where ψ^α is the specific Helmholtz free energy of the α -phase, defined by

$$\psi^\alpha = \varepsilon^\alpha - \theta \eta^\alpha. \quad (\text{A.12})$$

Consider that the temperature θ is continuous across Γ , that is, $[[\theta]] = 0$, in which case Γ is known as an ‘ideal’ singular interface (Liu, 1980). In this case, the jump condition on entropy, (A.8), can be written as

$$\left[\left[\sum_\alpha \mathbf{h}^\alpha \right] \right] \cdot \mathbf{n} = - \left[\left[\sum_\alpha \theta \rho^\alpha \eta^\alpha (\mathbf{v}^\alpha - \mathbf{v}_\Gamma) \right] \right] \cdot \mathbf{n}. \quad (\text{A.13})$$

Substituting (A.13) into (A.7) produces

$$\left[\left[\sum_\alpha \left[\sigma^{\alpha T} - \rho^\alpha \left(\varepsilon^\alpha - \theta \eta^\alpha + \frac{1}{2} (\mathbf{v}^\alpha - \mathbf{v}_\Gamma) \cdot (\mathbf{v}^\alpha - \mathbf{v}_\Gamma) \right) \mathbf{I} \right] (\mathbf{v}^\alpha - \mathbf{v}_\Gamma) \right] \right] \cdot \mathbf{n} = 0. \quad (\text{A.14})$$

Making use of the definitions in (A.11) and (A.12) into (A.14) results in the jump condition

$$\left[\left[\sum_\alpha - \left(\mathbf{K}^\alpha + \frac{1}{2} (\mathbf{v}^\alpha - \mathbf{v}_\Gamma) \cdot (\mathbf{v}^\alpha - \mathbf{v}_\Gamma) \mathbf{I} \right) \rho^\alpha (\mathbf{v}^\alpha - \mathbf{v}_\Gamma) \right] \right] \cdot \mathbf{n} = 0. \quad (\text{A.15})$$

For hydrated biological tissues, it is convenient to define material regions on the solid phase. Thus, jump interfaces can be represented with $\mathbf{v}_\Gamma = \mathbf{v}^s$. Furthermore,

for the fluid phases (e.g. water and ions), the dissipative stress is typically neglected (i.e. the fluid is assumed inviscid), so that $\boldsymbol{\sigma}^\alpha$, and hence \mathbf{K}^α , is an isotropic tensor ($\alpha \neq s$), for example,

$$\mathbf{K}^\alpha = \tilde{\mu}^\alpha \mathbf{I}, \quad (\text{A.16})$$

where $\tilde{\mu}^\alpha$ is the commonly defined electrochemical potential. Combining these results into (A.15), and accounting for (A.10) produces

$$\sum_{\alpha \neq s} \left[\left[\tilde{\mu}^\alpha + \frac{1}{2}(\mathbf{v}^\alpha - \mathbf{v}^s) \cdot (\mathbf{v}^\alpha - \mathbf{v}^s) \right] \right] \rho^\alpha (\mathbf{v}^\alpha - \mathbf{v}^s) \cdot \mathbf{n} = 0. \quad (\text{A.17})$$

Now recognizing that $\tilde{\mu}^\alpha + (\mathbf{v}^\alpha - \mathbf{v}^s) \cdot (\mathbf{v}^\alpha - \mathbf{v}^s)/2$ is independent of $\rho^\alpha (\mathbf{v}^\alpha - \mathbf{v}^s) \cdot \mathbf{n}$, the jump condition for the chemical potential of the α -phase reduces to

$$\left[\left[\tilde{\mu}^\alpha + \frac{1}{2}(\mathbf{v}^\alpha - \mathbf{v}^s) \cdot (\mathbf{v}^\alpha - \mathbf{v}^s) \right] \right] = 0, \alpha \neq s. \quad (\text{A.18})$$

If we also define the inner part of the total stress $\boldsymbol{\sigma}$ as the sum of the stresses from all phases,

$$\boldsymbol{\sigma} = \sum_{\alpha} \boldsymbol{\sigma}^\alpha, \quad (\text{A.19})$$

the linear momentum jump condition of (A.6) becomes

$$\left[\left[\boldsymbol{\sigma} - \sum_{\alpha} \rho^\alpha (\mathbf{v}^\alpha - \mathbf{v}^s) \otimes (\mathbf{v}^\alpha - \mathbf{v}^s) \right] \right] \cdot \mathbf{n} = \mathbf{0}. \quad (\text{A.20})$$

Equations (A.18) and (A.20) represent the generalization of the jump conditions summarized in Equation (13) above. They are valid for dynamic problems as well as steady-state equilibrium problems; they are based on the following assumptions: (a) there is no mass production at the jump interface; (b) the fluid phases are inviscid; and (c) the interface is non-dissipative (no frictional heat losses).

Hence, the use of the expressions in Equation (13) is appropriate under the assumptions outlined here. Dropping the higher order terms in the jump conditions is justified by an order of magnitude analysis, which is most commonly done in all problems of continuum mechanics. However, if the effect of frictional heat is to be accounted in the jump condition, more general expressions would be required which are not investigated here; furthermore, constitutive relations would be necessary to model the energy dissipation at the jump interface, for example, based on the formulation of a friction coefficient as proposed in this study, and temperature changes may have to be considered as well. This increased level of complexity may be addressed in future studies.

Acknowledgement

This study was supported in part by the National Institutes of Health (NIAMS AR43628, AR46532, AR46568, and AR41913).

References

- Armstrong, C. G., Mow, V. C. and Lai, W. M.: 1984, An analysis of unconfined compression of articular cartilage, *J. Biomech. Eng.* **106**, 165–173.
- Ateshian, G. A., Lai, W. M., Zhu, W. B. and Mow, V. C.: 1994, An asymptotic solution for two contacting biphasic cartilage layer, *J. Biomech.* **27**, 1347–1360.
- Ateshian, G. A. and Wang, H.: 1995, A theoretical solution for the rolling contact of frictionless cylindrical biphasic articular cartilage layers, *J. Biomech.* **28**, 1341–1355.
- Ateshian, G. A.: 1997, A theoretical formulation for boundary friction in articular cartilage, *J. Biomech. Eng.* **119**, 81–86.
- Ateshian, G. A., Wang, H. and Lai, W. M.: 1998, The role of interstitial fluid pressurization and surface porosities on the boundary friction of articular cartilage, *J. Tribol.* **120**, 241–251.
- Basser, P. J., Schneiderman, R., Bank, R. A., Wachtel, E. and Maroudas, A.: 1998, Mechanical properties of the collagen network in human articular cartilage as measured by osmotic stress technique, *Arch. Biochem. Biophys.* **15;351**, 207–219.
- Bowen, R. M.: 1980, Incompressible porous media models by use of the theory of mixtures, *Int. J. Eng. Sci.* **18**, 1129–1148.
- Curnier, A., He, Q.-C. and Zysset, P.: 1995, Conewise linear elastic materials, *J. Elast.* **37**, 1–38.
- Delesse, M. A.: 1847, Procédé mécanique pour déterminer la composition des roches, *C. R. Acad. Sci. (Paris)* **25**, 544.
- Dintenfuss, L.: 1963, Lubrication in synovial joints, *Nature (London)* **197**, 496–497.
- Dowson, D.: 1967, Modes of lubrication in human joints, *Proc. Inst. Mech. Eng. [H]* **181**, 45–54.
- Dowson, D. and Jin, Z.-M.: 1986, Micro-elastohydrodynamic lubrication of synovial joints, *Proc. Inst. Mech. Eng. [H] J. Eng. Med.* **15**, 63–65.
- Eisenberg, S. R. and Grodzinsky, A. J.: 1985, Swelling of articular cartilage and other connective tissues: electromechanochemical forces, *J. Orthop. Res.* **3**, 148–159.
- Farndale, R. W., Sayers, C. A. and Barrett, A. J.: 1982, A direct spectrophotometric microassay for sulfated glycosaminoglycans in cartilage cultures, *Connect. Tissue Res.* **9**, 247–248.
- Forster, H. and Fisher, J.: 1996, The influence of loading time and lubricant on the friction of articular cartilage, *Proc. Inst. Mech. Eng. [H]* **210**, 109–119.
- Frank, E. H. and Grodzinsky, A. J.: 1987, Cartilage electromechanics – II. A continuum model of cartilage electrokinetics and correlation with experiments, *J. Biomech.* **20**, 629–639.
- Gu, W. Y., Lai, W. M. and Mow, V. C.: 1998, A mixture theory for charged hydrated soft tissues containing multi-electrolytes: passive transport and swelling behaviors, *J. Biomech. Eng.* **120**, 169–180.
- Hills, B. A.: 1989, Oligolamellar lubrication of joints by surface active phospholipid, *J. Rheum.* **16**, 82–91.
- Hlavacek, M.: 1993, The role of synovial fluid filtration by cartilage in lubrication of synovial joints II. Squeeze-film lubrication: homogeneous lubrication, *J. Biomech.* **26**, 1151–1160.
- Hlavacek, M.: 2000, Squeeze-film lubrication of the human ankle joint with synovial fluid filtrated by articular cartilage with the superficial zone worn out, *J. Biomech.* **33**, 1415–1422.
- Hou, J. S., Holmes, M. H., Lai, W. M. and Mow, V. C.: 1989, Boundary conditions at the cartilage-synovial fluid interface for joint lubrication and theoretical verifications, *J. Biomech. Eng.* **111**, 78–87.
- Hou, J. S., Mow, V. C., Lai, W. M. and Holmes, M. H.: 1992, Squeeze film lubrication for articular cartilage with synovial fluid, *J. Biomech.* **25**, 247–259.
- Huyghe, J. M. and Janssen, J. D.: 1997, Quadriphasic mechanics of swelling incompressible porous media, *Int. J. Eng. Sci.* **35**, 793–802.
- Jin, Z. M., Dowson, D. and Fisher, J.: 1992, Effect of porosity of articular cartilage on the lubrication of a normal human hip joint, *Proc. Inst. Mech. Eng. [H] J. Eng. Med.* **206**, 117–124.

- Lai, W. M., Hou, J. S. and Mow, V. C.: 1991, A triphasic theory for the swelling and deformational behaviors of articular cartilage, *J. Biomech. Eng.* **113**, 245–258.
- Linn, F. C. and Sokoloff, L.: 1965, Movement and composition of interstitial fluid of cartilage, *Arthritis Rheum.* **8**, 481.
- Liu, I.-S.: 1980, On chemical potential and incompressible porous media, *J. de Mécanique* **19**(2), 327–342.
- Macirowski, T., Tepic, S. and Mann, R. W.: 1994, Cartilage stresses in the human hip joint, *J. Biomech. Eng.* **116**, 11–18.
- MacConaill, M. A.: 1932, The function of intra-articular fibrocartilages, with special references to the knee and inferior radio-ulnar joints, *J. Anat.* **66**, 210–227.
- Mak, A. F., Lai, W. M. and Mow, V. C.: 1987, Biphasic indentation of articular cartilage: Part I. Theoretical analysis, *J. Biomech.* **20**, 703–714.
- Malcom, L. L.: 1976, An experimental investigation of the frictional and deformational responses of articular cartilage interfaces to static and dynamic loading, PhD Thesis, University of California, San Diego.
- Maroudas, A.: 1968, Physicochemical properties of cartilage in the light of ion exchange theory, *Biophys. J.* **8**, 575–595.
- Maroudas, A.: 1979, Physicochemical properties of articular cartilage, In: M. A. R. Freeman (ed.), *Adult Articular Cartilage*, 2nd edn., Tunbridge Wells, England, Pitman Medical, pp. 215–290.
- McCutchen, C. W.: 1962, The frictional properties of animal joints, *Wear* **5**, 1–17.
- McCutchen, C. W.: 1966, Boundary lubrication by synovial fluid: demonstration and possible osmotic explanation, *Fed. Proc.* **25**, 1061–1068.
- Mow, V. C., Kuei, S. C., Lai, W. M. and Armstrong, C. G.: 1980, Biphasic creep and stress relaxation of articular cartilage in compression: theory and experiments, *J. Biomech. Eng.* **102**, 73–84.
- Narmoneva, D. A., Wang, J. Y. and Setton, L. A.: 1999, Nonuniform swelling-induced residual strains in articular cartilage, *J. Biomech.* **32**, 401–408.
- Seibel, M. J., Macauley, W., Jelsma, R., Saed-Nejad, F. and Ratcliffe, A.: 1992, Antigenic properties of keratan sulfate: influence of antigen structure, monoclonal antibodies, and antibody valency, *Arch. Biochem. Biophys.* **296**, 410–418.
- Soltz, M. A. and Ateshian, G. A.: 1998, Experimental verification and theoretical prediction of cartilage interstitial fluid pressurization at an impermeable contact interface in confined compression, *J. Biomech.* **31**, 927–934.
- Soltz, M. A. and Ateshian, G. A.: 2000a, Interstitial fluid pressurization during confined compression cyclical loading of articular cartilage, *Ann. Biomed. Eng.* **28**, 150–159.
- Soltz, M. A. and Ateshian, G. A.: 2000b, A conewise linear elasticity mixture model for the analysis of tension-compression nonlinearity in articular cartilage, *J. Biomech. Eng.* **122**, 576–586.
- Swann, D. A. and Radin, E. L.: 1972, The molecular basis of articular lubrication: I. Purification and properties of a lubricating fraction from bovine synovial fluid, *J. Biol. Chem.* **247**, 8069–8073.
- Swann, D. A., Radin, E. L. and Hendren, R. B.: 1979, The lubrication of articular cartilage by synovial fluid glycoproteins, *Arthritis Rheum.* **22**, 665–666.
- Tanner, R. I.: 1966, An alternative mechanism for the lubrication of synovial joints, *Phys. Med. Biol.* **11**, 119–127.
- Unsworth, A., Dowson, D. and Wright, V.: 1975, The frictional behavior of human synovial joints: I. Natural joints, *J. Lubr. Technol.* **97**, 360–376.
- Wang, H. and Ateshian, G. A.: 1997, The normal stress effect and equilibrium friction coefficient of articular cartilage under steady frictional shear, *J. Biomech.* **30**, 771–776.
- Wright, V. and Dowson, D.: 1976, Lubrication and cartilage, *J. Anat.* **121**, 107–118.